AMERICAN SOCIETY FOR MICROBIOLOGY | mBio®

RESEARCH ARTICLE

Characterization of a Pathogenic Full-Length cDNA Clone and Transmission Model for Porcine Epidemic Diarrhea Virus Strain PC22A

Anne Beall,[a] Boyd Yount,[a] Chun-Ming Lin,[b] Yixuan Hou,[b] Qiuhong Wang,[b] Linda Saif,[b] Ralph Baric[a]

University of North Carolina Chapel Hill, Chapel Hill, North Carolina, USA[a]; Food Animal Health Research Program, Ohio Agricultural Research and Development Center, The Ohio State University, Wooster, Ohio, USA[b]

ABSTRACT **Porcine epidemic diarrhea virus (PEDV) is a highly pathogenic alphacoronavirus. In the United States, highly virulent PEDV strains cause between 80 and 100% mortality in suckling piglets and are rapidly transmitted between animals and farms. To study the genetic factors that regulate pathogenesis and transmission, we developed a molecular clone of PEDV strain PC22A. The infectious-clone-derived PEDV (icPEDV) replicated as efficiently as the parental virus in cell culture and in pigs, resulting in lethal disease *in vivo*. Importantly, recombinant PEDV was rapidly transmitted to uninoculated pigs via indirect contact, demonstrating virulence and efficient transmission while replicating phenotypes seen in the wild-type virus. Using reverse genetics, we removed open reading frame 3 (ORF3) and replaced this region with a red fluorescent protein (RFP) gene to generate icPEDV-ΔORF3-RFP. icPEDV-ΔORF3-RFP replicated efficiently *in vitro* and *in vivo*, was efficiently transmitted among pigs, and produced lethal disease outcomes. However, the diarrheic scores in icPEDV-ΔORF3-RFP-infected pigs were lower than those in wild-type-virus- or icPEDV-infected pigs, and the virus formed smaller plaques than those of PC22A. Together, these data describe the development of a robust reverse-genetics platform for identifying genetic factors that regulate pathogenic outcomes and transmission efficiency *in vivo*, providing key infrastructural developments for developing and evaluating the efficacy of live attenuated vaccines and therapeutics in a clinical setting.**

IMPORTANCE **Porcine epidemic diarrhea virus (PEDV) emerged in the United States in 2013 and has since killed 10% of U.S. farm pigs. Though the disease has been circulating internationally for decades, the lack of a rapid reverse-genetics platform for manipulating PEDV and identifying genetic factors that impact transmission and virulence has hindered the study of this important agricultural disease. Here, we present a DNA-based infectious-clone system that replicates the pathogenesis of circulating U.S. strain PC22A both *in vitro* and in piglets. This infectious clone can be used both to study the genetics, virulence, and transmission of PEDV coronavirus and to inform the creation of a live attenuated PEDV vaccine.**

Received 26 August 2015 **Accepted** 10 November 2015 **Published** 5 January 2016

Citation Beall A, Yount B, Lin C-M, Hou Y, Wang Q, Saif L, Baric R. 2016. Characterization of a pathogenic full-length cDNA clone and transmission model for porcine epidemic diarrhea virus strain PC22A. 7(1):e01451-15. doi:10.1128/mBio.01451-15.

Editor W. Ian Lipkin, Columbia University

Address correspondence to Ralph Baric, rbaric@email.unc.edu.

Coronaviruses are important emerging viruses that are capable of producing sudden pandemic disease outbreaks with high morbidity, mortality, and economic losses in animal and human populations (1). Porcine epidemic diarrhea virus (PEDV) is an alphacoronavirus that recently emerged in the United States and has since killed >8 million piglets, nearly 10% of all U.S. farm piglets in 2014 (2). In the United States, newly emerged strains of PEDV are highly virulent and cause mortality rates in suckling piglets of between 80 and 100% (2). Clinically, pigs infected with PEDV have severe diarrhea and vomiting, leading to death by dehydration within a few days of infection (2–4). PEDV readily spreads by fecal-oral transmission routes between swine, in swine feed, and through contaminated farming and transport equipment (5). A second newly discovered swine coronavirus in the United States, designated swine deltacoronavirus (SDCV), was discovered in Ohio and found to be closely related to coronaviruses detected in Hong Kong in 2012 (6). Porcine orthoreoviruses that are similar to strains identified in Southeast Asia have also been detected in U.S. herds (7). It is clear that new approaches are desperately needed to control pandemic outbreaks of swine respiratory and enteric viruses.

Although the origins of PEDV remain obscure and early sequence studies had suggested similarity to human coronavirus NL63, more-recent studies argue that PEDV is more closely related to several bat alphacoronaviruses identified in the United States, South America, and Eurasia (8, 9). PEDV first emerged in Europe in the 1970s and spread across Europe and into Asia (10). However, it was not until late 2010 that extremely virulent forms emerged in China (11). In the United States, phylogenetic studies suggest that PEDV is most closely related to Chinese strain AH2012*, although its transmission route to the United States still remains uncertain (2, 8, 12). Since the first U.S. outbreak of PEDV in April 2013, PEDV has rapidly spread across 34 states, Canada, and Central America and has returned to devastate the swine in-

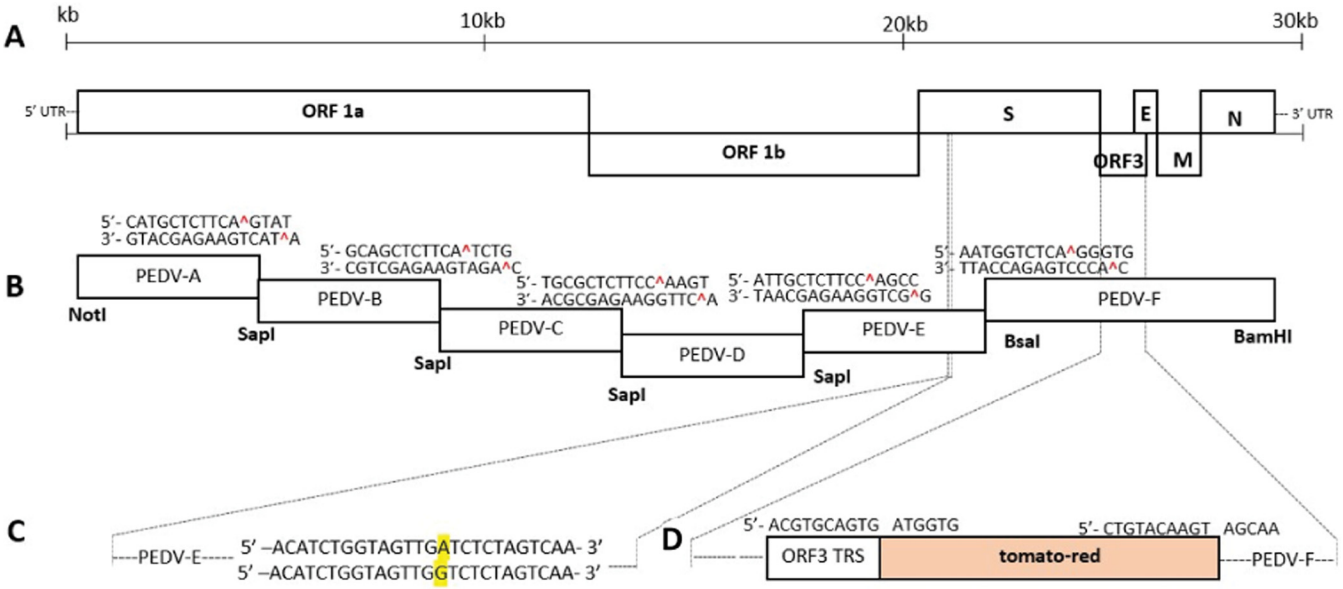

FIG 1 Schematic of the full-length PEDV genome and construction of the infectious PEDV cDNA clone and mutants. (A) PEDV genome, including ORF1a, ORF1b, and the spike (S), ORF3, envelope (E), membrane (M), and nucleocapsid (N) genes. (B) cDNA fragments comprising icPEDV. Restriction sites joining fragments are noted. (C) The BsaI site was removed from icPEDV, as indicated by the A to G nucleotide change in yellow. (D) PEDV-ΔORF3-RFP. Restriction sites were used to replace ORF3 with tomato-red and the ORF3 transcription regulatory sequence (TRS). 5′ and 3′ UTR, 5′ and 3′ untranslated regions.

dustry in Asia (13, 14). During this ongoing outbreak, new strategies are desperately needed to understand pathogenic mechanisms and the functions of viral genes and to provide new technologies to combat this disease.

PEDV appears to recognize CD13, an aminopeptidase N protein, as a receptor for entry into pig cells, as well as the sugar coreceptors heparan sulfate and *N*-acetylneuraminic acid (15, 16). PEDV can infect multiple cell types *in vitro*, including swine, human, primate, and bat cells, suggesting the possibility of adaptation and spread to other species (15). The PEDV genome is composed of 28,000 nucleotides (nt) encoding seven known open reading frames (ORFs) expressed from both genomic and subgenomic mRNAs (17). Subgenomic mRNAs are arranged in a nested fashion from the 3′ end of the genome. PEDV encodes the traditional coronavirus structural proteins: a receptor-binding spike glycoprotein (S), the envelope protein (E), the membrane glycoprotein (M), and the nucleocapsid protein (N). The spike glycoprotein is a type I membrane glycoprotein composed of S1 and S2 external domains, a transmembrane domain, a C-terminal cytoplasmic domain, and a signal peptide. The S protein plays a role in virulence, growth adaptation, receptor binding, and virus-cell membrane fusion (18, 19). E of PEDV (PEDV-E) upregulates stress pathways in the host cell, induces antiapoptotic factors, and is important for viral budding (20). PEDV-N induces cell stress and prevents apoptosis through similar pathways and prolongs the host cell's S phase (21). Additionally, PEDV contains at least three additional ORFs: ORF1a, ORF1b, and ORF3. ORF1a and -b encode two viral proteases that process these large precursor polyproteins into 16 nonstructural proteins, including the viral replicase and associated RNA-modifying enzymes that are critical for full-length and subgenomic positive- and negative-strand RNA synthesis (22). ORF3 regulates virus production and encodes an ion channel important for viral fitness but is not required for viral replication *in vitro* (23, 24).

In this study, we generated the first infectious cDNA clone of a virulent North American PEDV strain, PC22A (25). Parental genomic and ORF3 deletion recombinant viruses were generated using the infectious cDNA clone system; the latter was also engineered to express red fluorescent protein (RFP). Both recombinant viruses are replication competent *in vitro* and pathogenic in neonatal gnotobiotic (Gn) piglets. Parental and recombinant viruses were efficiently transmitted to uninoculated pigs via indirect contact, allowing for genetic studies into the molecular mechanisms regulating virus transmission and pathogenesis. The availability of an infectious clone for PEDV will allow us further opportunities to understand gene function and genetic variants in PEDV pathogenesis and transmission, leading to better-informed design of vaccines and therapeutics.

RESULTS

Design of an infectious PEDV clone. We have developed molecular clones for several highly pathogenic swine and human coronaviruses, using class II restriction endonucleases, to directionally assemble a full-length cDNA viral genome from a set of sequentially designed smaller cDNAs (26–31). To develop a molecular clone for PEDV, the highly virulent PC22A strain (Fig. 1A) was sequenced and synthesized as six contiguous PEDV subclones designated A to F (Fig. 1B). Subclones A/B, B/C, C/D, and D/E are joined by unique SapI restriction endonuclease cleavage sites (at nucleotide positions 4071, 8287, 12016, and 16941, respectively) that allow for directional assembly into a full-length cDNA without alteration of the viral amino acid sequence. Subclones E and F are joined at a unique BsaI site at nucleotide position 22504. In subclone F, a single BsaI restriction site in PEDV-PC22A was removed by introducing a silent mutation at position 24337, effectively marking the recombinant genome (Fig. 1C). Thus, each fragment contains a unique set of class II restriction enzyme sites flanking the genomic sequence that allow for unique 3-nt over-

hangs between each fragment. This specificity allows for systematic, efficient, and directional assembly of the complete PEDV genome by *in vitro* ligation. The PEDV A fragment contains a T7 start site, whereas the F fragment terminates in 22 A residues, allowing for *in vitro* transcription and capping of a polyadenylated full-length transcript.

PEDV-ORF3 is an accessory ORF encoding a putative ion channel protein that is oftentimes deleted from some natural isolates or following *in vitro* passage, suggesting that it encodes nonessential functions *in vitro* and/or *in vivo* (24). To generate a fluorescently marked PEDV genome mutant, ORF3 in the PEDV F fragment was replaced with red fluorescent protein (RFP), named tomato-red (Fig. 1D). The mutant was created using native restriction enzyme recognition sequences that allowed for the preservation of the ORF3 transcription regulatory sequence (TRS), which regulates subgenomic RNA expression (Fig. 1D).

Recovery of recombinant viruses. To isolate recombinant wild-type and RFP-expressing recombinant PEDVs, each plasmid fragment was digested with noted restriction enzymes, purified, and ligated to create a full-length PEDV cDNA genome. Using the T7 RNA polymerase, full-length transcripts were synthesized *in vitro* as previously described by our group (26, 30). As previous swine and human coronavirus infectious clones displayed improved recovery rates and replication efficiency in the presence of the supplemented N gene transcript (26, 30), capped PEDV-N gene transcripts were mixed with the full-length genomic transcripts prior to their electroporation into Vero cells. Within 24 to 48 h postelectroporation, subgenomic recombinant-virus mRNA could be detected via reverse transcription-PCR (RT-PCR). After we isolated recombinant virus from pig intestinal contents after inoculation, wild-type and recombinant viruses replicated to titers that approached or exceeded 1×10^4 PFU/ml in Vero cells, equivalent to titers commonly reported in the literature (Fig. 2A). A recombinant infectious-clone-derived PEDV (icPEDV) produced a plaque morphology (Fig. 2B) similar to that of the parental strain and formed syncytia characteristic of PEDV in culture (Fig. 2C). Notably, icPEDV-ΔORF3-RFP displayed a reduced plaque size compared to that of either PC22A or icPEDV (Fig. 2B), indicative that ORF3 may be important for *in vitro* growth of the virus and suggestive of possible attenuation of the ORF3 deletion mutant. At 48 and 72 h postelectroporation with icPEDV-ΔORF3-RFP, fluorescent red cells were seen in cell culture, both within individual cells and within larger syncytia (Fig. 2D).

Characterization of recombinant viruses. To evaluate protein expression in our recombinant PEDV, we cloned and expressed PEDV-S and PEDV-N in Venezuelan equine encephalitis virus strain 3526 virus replicon particles (VRP) and isolated VRP-PEDV-S and VRP-PEDV-N. The VRP were inoculated into the footpads of mice, and polyclonal PEDV-N and PEDV-S antisera were collected after a day 21 boost. Using Western blot techniques, we confirmed the presence of the 180-/90- and ~50-kDa PEDV-S and PEDV-N proteins, respectively, in cells infected with icPEDV, icPEDV-ΔORF3-RFP, and parental PEDV *in vitro* (Fig. 3A). Thus, molecularly derived viruses have protein expression phenotypes similar to those of the parental virus.

To further confirm the presence of the recombinant virus postelectroporation, we reverse transcribed genomic RNA from virions in the culture media and then sequenced them to demonstrate the presence of the distinguishing BsaI cloning site in infectious-clone viruses (Fig. 3B). Additionally, we sequenced the leader-containing subgenomic mRNA transcripts to ensure that both our recombinant viruses and their parental strain shared the wild-type transcription regulatory sequence (TRS) required for normal coronavirus replication and growth kinetics (Fig. 3C). Together, these data definitively demonstrate that both recombinant clones generated replicating recombinant virus *in vitro*.

icPEDV replication and pathogenesis in Gn piglets. PEDV PC22A is highly pathogenic in newborn piglets and is rapidly transmitted to littermates. To determine if icPEDV replicated parental PEDV PC22A *in vivo* pathology and transmission phenotypes, gnotobiotic (Gn) pigs were orally inoculated with icPEDV (passage 0 [P0]), icPEDV-ΔORF3-RFP (P0), or PC22A (P3) and housed with uninfected indirect-contact pigs (Table 1). Challenged animals demonstrated fecal viral RNA shedding, and diarrhea started 1 to 3 days postinfection (dpi) in all three virus groups (Fig. 4A; Table 1). Importantly, uninoculated indirect-contact pigs within each group demonstrated both robust virus shedding and diarrhea, confirming the transmissibility of both PC22A and the recombinant virus (Fig. 4B). All three viruses replicated to similar peak titers (11 to 13 $\log_{10}$ genomic equivalents [GE]/ml). However, PC22A and icPEDV group pigs had more-severe diarrhea (highest fecal score of 3) than icPEDV-ΔORF3-RFP group pigs (highest score of 2). The day of harvest for each piglet was dependent on clinical fecal scores or occurred upon the death of the piglet. Notably, days of harvest varied both between virus types and within virus groups. Because of the animal numbers in each group and because of the variation within each PEDV group, the day of harvest cannot be used as a reliable indicator of the relative degree of viral virulence or attenuation. The pathogenesis of icPEDV in Gn pigs also replicated the pathogenic phenotype of PEDV strain PC21A, which had been collected from the same swine farm on the same day as PC22A (4).

Histopathological examination showed severe villous atrophy in PEDV PC22A- and icPEDV-inoculated pigs and moderate-to-severe villous atrophy in icPEDV-ΔORF3-RFP-infected pigs (Fig. 5A). The villous height/crypt depth (VH/CD) ratio of the jejunum of a mock-inoculated pig was significantly higher than those of PC22A-, icPEDV-, and icPEDV-ΔORF3-RFP-infected pigs ($P < 0.05$) (Table 1). Immunohistochemistry (IHC) for PEDV-N confirmed the presence of recombinant virus throughout the small intestine (duodenum, jejunum, and ilium) in both icPEDV- and icPEDV-ΔORF3-RFP-infected pigs (Fig. 5B; Table 2). In addition, icPEDV antigens were detected in the large intestine (colon).

These results indicate that the cell culture supernatants of icPEDV and icPEDV-ΔORF3-RFP contained infectious recombinant virus particles that replicated well in gnotobiotic pigs. While the recombinant icPEDV replicated the clinical phenotypes of parental PC22A *in vivo*, icPEDV-ΔORF3-RFP infection resulted in a partial attenuation in pigs based on lower diarrhea scores. The rapid infection of contact pigs suggests efficient transmission of icPEDV and icPEDV-ΔORF3-RFP, replicating both parental PC22A and circulating U.S. strain transmission phenotypes.

DISCUSSION

Emerging viruses pose a considerable threat to humans and society by causing morbidity and mortality in human populations or causing significant losses in important food sources and trade,

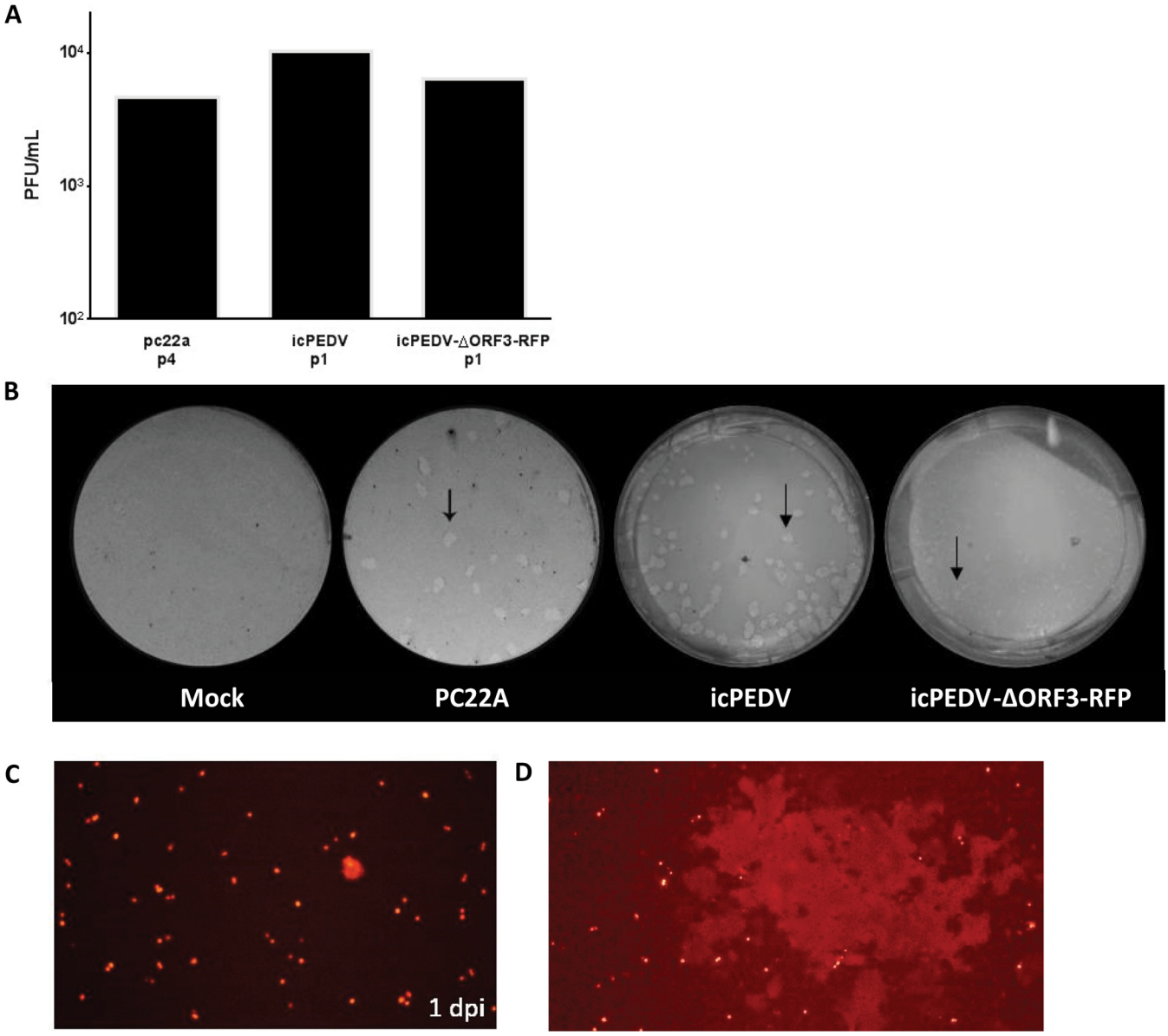

FIG 2 Growth of icPEDV clones isolated from *in vivo* small intestine samples. (A) Titers of viral stocks isolated from small intestinal contents at the noted passages, harvested 2 dpi; (B) representative plaques (arrows) of mock-infected cells and cells infected with the parental PC22A strain, icPEDV, and icPEDV-ΔORF3-RFP, from left to right, at 2 dpi; (C) fluorescence microscopy of passage 0 icPEDV-ΔORF3-RFP in cell culture at 1 dpi; (D) syncytium formation of passage 0 icPEDV-ΔORF3-RFP.

leading to economic instability and loss of critical protein sources, especially in poor rural populations. Porcine epidemic diarrhea virus is a serious livestock pathogen that is causing significant economic losses in the swine industry internationally. To date, over a billion piglets have died globally. Live vaccine has been used historically to combat PEDV outbreaks in Asia; however, live vaccines available today are ineffective in preventing outbreaks of circulating pandemic strains, including U.S. outbreak strains, and have not significantly reduced the global disease burden (14). Other important nidovirus infections of swine include transmissible gastroenteritis virus (TGEV), its related respiratory variant designated porcine respiratory coronavirus (PRCV), and porcine reproductive and respiratory disease virus (PRRSV), which have caused major economic losses to the swine industry since the late 1980s (32–34). In addition to PEDV, an emerging coronavirus, porcine deltacoronavirus, has recently been reported in swine, demonstrating the possibility of continued emergent threats to this important food industry (6, 35). Given the apparent increase in the number of new swine viruses identified over the past 30 years, it seems clear that management practices and/or other changes in the ecosystem are providing an environmental setting that promotes the emergence of new viral pathogens for the swine industry. If so, these data document the need for the development of new, rapid-response intervention platforms for disease control in critical livestock populations that are centrally linked to human health. In this article, we describe the first molecular clone for a

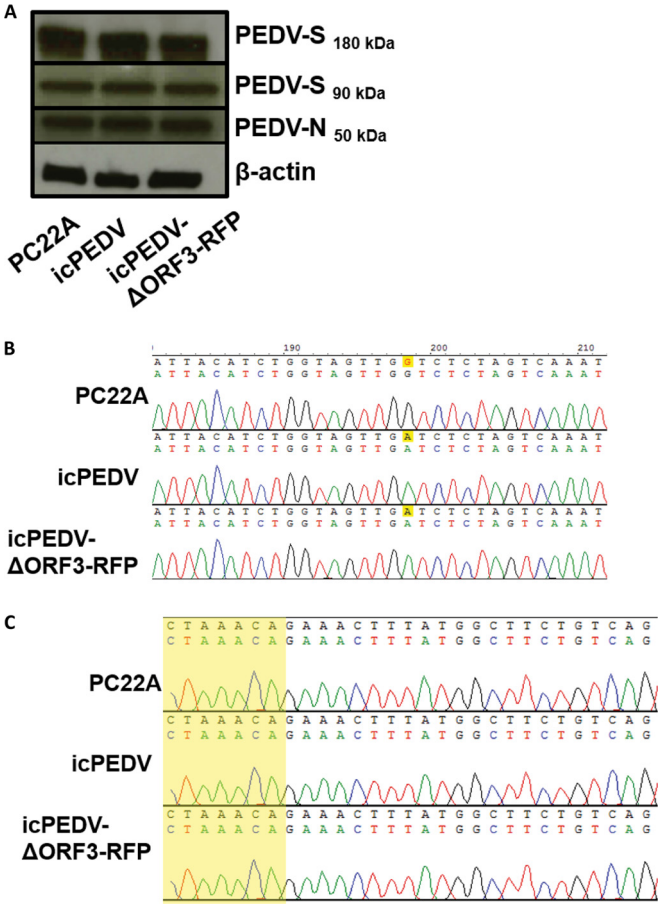

FIG 3 Confirmatory studies of the infectious PEDV clone. (A) Western blot for PEDV spike (PEDV-S), before (180 kDa) and after (90 kDa) cleavage with trypsin, and nucleocapsid (PEDV-N). Protein was isolated from Vero cells infected with PC22A, icPEDV, or icPEDV-ΔORF3-RFP, which was harvested and sequenced 2 dpi. (B) An altered BsaI cloning site is conserved (yellow highlighting) after viral passage in piglets. (C) The transcription regulatory sequence (TRS) in the leader region of PEDV subgenomic transcripts is conserved between the wild type and icPEDV. The sequence is highlighted in yellow.

highly pathogenic U.S. strain of PEDV, PC22A, isolated from an outbreak in Ohio in June 2013 (25). Both the parental PEDV PC22A strain and its derivative recombinant cloned virus were genetically stable and fully pathogenic in neonatal gnotobiotic pigs, demonstrating that icPEDV provides not only a strategy that allows for the systematic evaluation of the role of viral genes in pathogenesis, tropism, and virulence but also a translational platform for the development of rationally attenuated live virus vaccines. In addition, we have constructed a recombinant PEDV that bears an indicator gene, the RFP gene, which allows for rapid evaluation of antiviral efficacy and neutralizing antibody levels by means of high-throughput cell culture systems.

Recently, a molecular clone for a high-growth tissue culture variant of a 2010 Thai isolate, designated $PEDV_{AVCT12}$, was reported in the literature (36). In contrast to our findings, full-length recombinant $PEDV_{AVCT12}$ could not be isolated unless ORF3 expression had been ablated, either by naturally occurring deletions or by insertion of an indicator gene in this location. Interestingly, naturally occurring deletions also removed 7 amino acids from the C terminus of the S protein, similar to deletions described with other tissue culture strains, like PEDV strain CHM2013 (36). At this time, the discrepancy between the two laboratory results is intriguing and most likely is directly related to the backbone sequence of the two isolates and/or the difficulties associated with culturing clinical isolates of PEDV *in vitro*. Tissue culture $PEDV_{AVCT12}$ replicates 2 to 3 logs more efficiently than wild-type PEDV PC22A and icPEDV in culture, and trypsin is also required to culture the latter isolates *in vitro*. Future studies may well reveal the emergence of similar tissue culture adaptations during serial passage of our highly virulent PEDV PC22A and icPEDV in culture. Importantly, pathogenic outcomes *in vivo* were not evaluated using the heavily tissue culture-adapted $PEDV_{AVCT12}$ strain, so the utility of this recombinant virus in evaluating pathogenic outcomes and/or the role of tissue culture-adaptive mutations in virulence are uncertain at best. Although an exact infectious dose of our recombinant viruses was not determined from these studies, <1 PFU of PEDV PC22A is sufficient to cause disease in piglets (37).

Little information is available regarding the molecular mecha-

TABLE 1 Summary of PEDV replication and pathogenesis in Gn pigs[b]

Group	No. of pigs	Pig	Age at inoculation (days)	Inoculation or contact[a]	Onset of fecal RNA shedding/diarrhea (dpi or dpc)	Highest fecal score[c]/ fecal RNA shedding titer (GE/ml)	Age (dpi) of piglet at euthanasia (day)	Jejunum VH/CD ratio
icPEDV	5	1	19	Inoculation	2/2	3/12.9	ND	ND
		2	19	Contact	2/4	3/13.2	24 (5)	1.2 ± 0.2
		3	16	Inoculation	1/2	3/11.5	20 (4)	1.4 ± 0.2
		4	16	Inoculation	1/2	3/12.0	21 (5)	1.3 ± 0.2
		5	16	Contact	1/2	3/11.5	21 (5)	3.1 ± 1.5
icPEDV-ΔORF3-RFP	3	6	14	Inoculation	1/1	2/11.6	16 (2)	2.2 ± 0.1
		7	14	Contact	2/5	2/11.6	21 (7)	1.0 ± 0.0
		8	14	Inoculation	1/3	2/10.8	17 (3)	2.7 ± 0.4
PC22A	4	9	18	Inoculation	1/1	3/13.0	19 (1)	1.4 ± 0.3
		10	18	Contact	2/3	3/11.8	21 (3)	1.3 ± 0.1
		11	26	Inoculation	1/1	3/11.8	27 (3)	ND
		12	26	Contact	1/2	3/11.12	21 (7)	ND
Mock infected	1	11	NA	NA	NA	1/NA	19	6.8 ± 0.9

[a] Pigs 2, 5, 7, and 10 were exposed by indirect contact to the pigs which were housed in the same isolator through small holes drilled into the stainless steel divider. The panel was located between the 2 pigs in the shared pig tub isolator unit.

[b] ND, not done because pig 1 was used for hyperimmune serum production; NA, not available; VH/CD, villous height/crypt depth.

[c] Fecal scores were as follows: 0, normal; 1, pasty stool; 2, semiliquid diarrhea; and 3, liquid diarrhea.

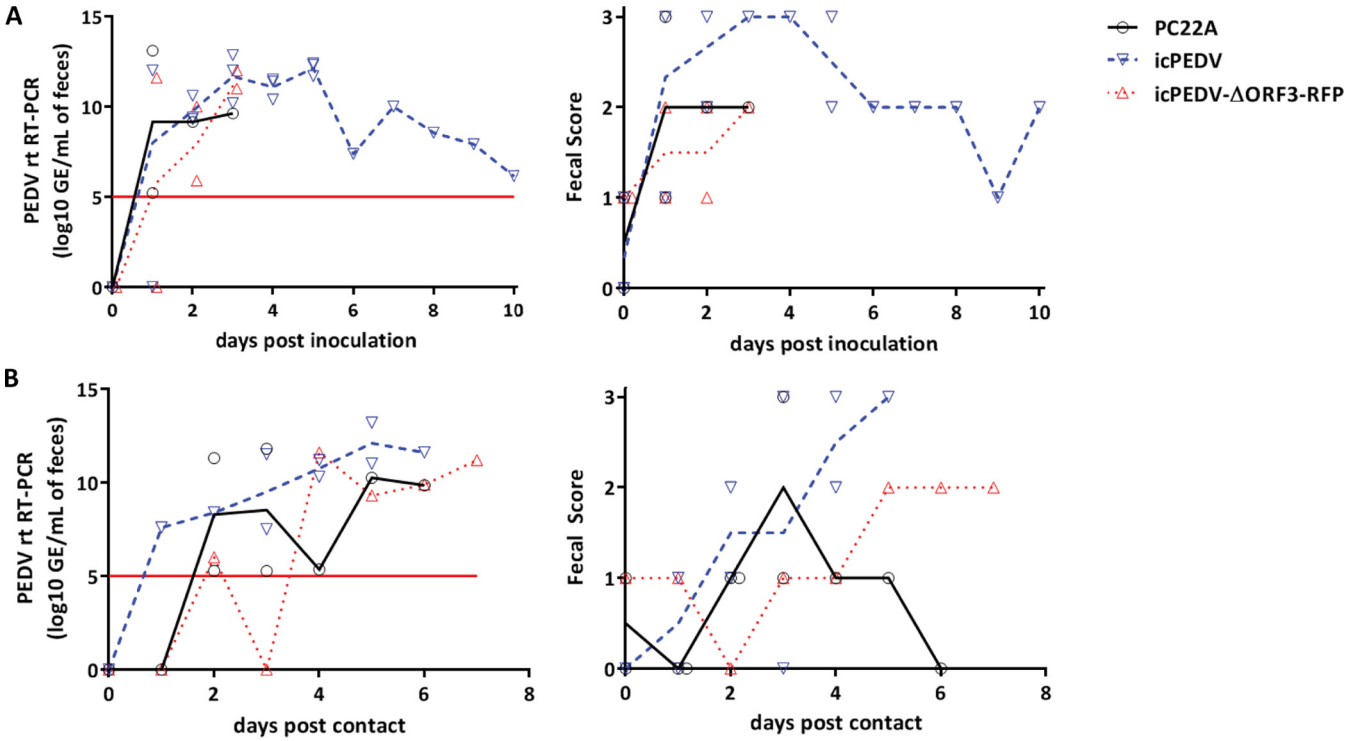

FIG 4 icPEDV mimics wild-type PEDV infection in gnotobiotic piglets. Gnotobiotic piglets were infected orally with 2 ml of the PEDV supernatant, and an uninoculated piglet was cohoused with them to determine transmission. All animals succumbed to illness or were euthanized due to illness at their final time points. (A) Mean RT-qPCR titers of fecal samples and fecal scores after viral inoculation. The line represents mean values, with individual piglet values shown by points. (B) RT-qPCR titers of fecal samples and fecal scores in cohoused transmission control piglets, days after contact with the inoculated piglets whose results are represented in panel A. The limit of detection in real-time (rt) RT-PCR figures (threshold cycle 37) is represented by a red line.

nisms governing efficient coronavirus pathogenesis and transmission between hosts. Importantly, icPEDV and icPEDV-ΔORF3-RFP are efficiently transmitted to cohoused littermates, providing a potential platform for investigating the genetic mechanisms regulating efficient transmission between hosts. While similar studies using highly pathogenic influenza viruses in ferrets are highly controversial because of potential human-pandemic concerns (38), identifying genetic factors that attenuate transmission frequency offer a powerful tool to improve the safety and efficacy of live attenuated coronavirus vaccines, especially given the high-animal-density manufacturing approaches used in the swine industry. Such studies may also provide significant insights into the fundamental principles and genetic functions that influence the transmission efficiency of other highly pathogenic human coronaviruses, like severe acute respiratory syndrome coronavirus (SARS-CoV) and Middle East respiratory syndrome coronavirus (MERS-CoV).

PEDV infection is most devastating in neonatal and suckling piglets, necessitating vaccines that target lactogenic immunity through the vaccination of pregnant sows and gilts. Piglets do not attain passive immunity preparturition but instead receive IgG- and IgA-based lactogenic immunity from colostrum and milk, respectively. With both TGEV and PEDV, sows infected with live virulent virus transferred more protective immunity against viral challenge in their nursing piglets than sows infected with attenuated or inactivated virus (39). The USDA has granted conditional licenses to two PEDV manufacturers to date. The Harris vaccine uses an attenuated Venezuelan equine encephalitis virus (VEEV) vaccine strain replicon particle expressing the PEDV spike protein (40). The second is a parenterally killed virus vaccine made by Zoetis (41). Both are used to immunize pregnant sows and gilts. Their efficacy and ability to protect against various circulating U.S. strains are still under evaluation. We note that the VRP platform described in our paper was based on a biosafety level 2 (BSL2) nonselect agent, a VEEV strain designated 3526, which has been used in animal and human trials (42–44). In contrast to other VEEV replicon platforms, VEEV 3526 retains wild-type E1 and E2 glycoproteins, which efficiently target dendritic cells (45, 46), but lacks E3 sequences. This deletion of E3 confers an attenuated phenotype *in vivo*. VEEV 3526 expressing appropriate S glycoprotein genes provides robust protection against other coronaviruses, like SARS-CoV, MERS-CoV, and HKU5-S (47–49). Using VEEV 3526 structural genes allows for recovery of high-titer VRP encoding PEDV-S and/or -N under BSL2 conditions. It remains unclear whether the VRP 3526 platform will prove sufficiently robust to induce in sows lactogenic immunity capable of protecting suckling piglets (49). Future experiments will have to be designed and implemented to test the relative efficacies of VRP vaccines, killed-whole-virus vaccines, or future live attenuated-virus vaccines.

Importantly, no live-virus vaccine is currently available in the United States, and historical live vaccines have not been effective in combating current U.S. or Asian strains (14). Robust studies using SARS-CoV have identified several viral genes, including the E protein, the ExoN nsp14 RNA proofreading machinery, and the 2-*O*-methyltransferase nsp16 replicase, as high-priority targets for rational attenuation of coronaviruses (50–52). Because coronavi-

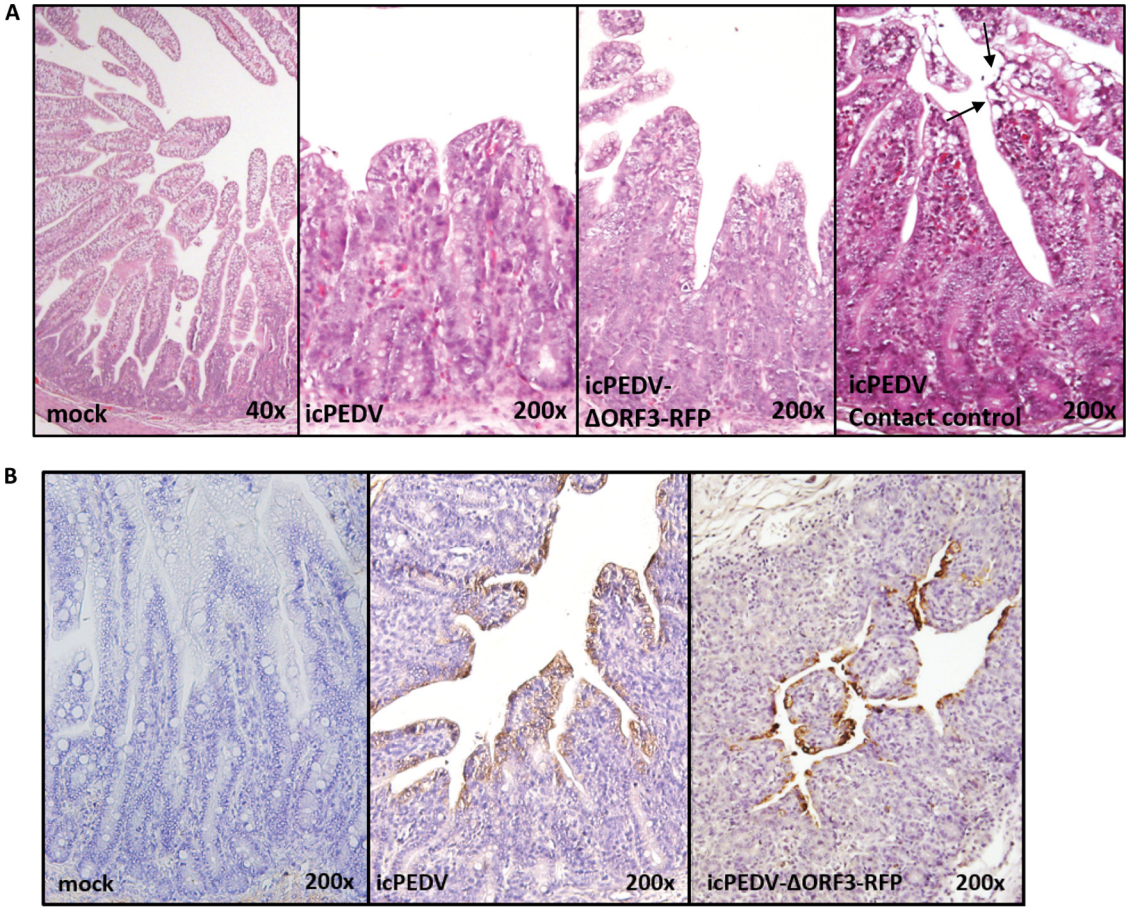

FIG 5 Histology and IHC staining of icPEDV-infected pig intestine. Gnotobiotic piglets were orally inoculated with 2 ml of PEDV. A contact control piglet was cohoused with an inoculated piglet(s) to determine transmission. All animals succumbed to illness or were euthanized due to illness at their final time points (PEDV, 1 dpi; icPEDV, 4 dpi; icPEDV-ΔORF3-RFP, 7 dpi; contact control, 4 dpi). All images show representative histological slides of jejunum specimens from mock-infected or infected animals. Histology of mock-, icPEDV-, or icPEDV-ORF3-RFP-infected animals, showing H&E staining and immunohistochemistry (IHC) staining (B) for PEDV nucleocapsid (N) protein using mouse anti-PEDV-N. A specimen from a contact piglet infected by icPEDV is also shown. Cell fusion and vacuolation were noted at the villus tips (arrows). IHC staining of icPEDV- or icPEDV-ΔORF3-RFP-infected animals whose results are represented in panel A is shown.

ruses undergo RNA recombination at high frequency and encode an exonuclease function (53, 54), recombination repair and reversion to wild-type virus is a pressing concern when designing live attenuated coronavirus vaccines. However, our laboratory has developed strategies to prevent recombination repair that limit the capacity of rationally designed live attenuated virus to revert to the wild-type virus sequence (55). Effective vaccines are increasingly important, as new strains are identified in the United States and circulating strains continue to devastate herds. The infectious clone platform allows for rapid construction of genetically modified PEDV variants to evaluate the function of antigenic variation on neutralization phenotypes and can be used for the rational design of a live virus vaccine. This platform also allows for incorporation of genetic changes to enhance the replication of the virus *in vitro* for more efficient production of attenuated vaccines. Globally, humans have experienced coronavirus outbreaks with increasing frequency, including outbreaks of two new human coronaviruses in the last 15 years, notably, SARS-CoV and MERS-CoV (56). Human and animal coronaviruses share similar structural proteins and replication dynamics. Currently, no transmission model for these important human pathogens is available. The neonatal pig model described in this study can provide a surrogate transmission model for human coronaviruses. Separately, the study of coronavirus transmission in its original host in a BSL2 climate affords the opportunity to safely and accurately research a

TABLE 2 Summary of IHC staining in infected pigs

Group	Pig	dpi	IHC signal intensity score[a]			
			Duodenum	Jejunum	Ileum	Colon
icPEDV	2	5	0	3	3	1
	3	4	2	3	3	1
	4	5	1	3	2	2
	5	5	1	3	2	1
icPEDV-ΔORF3-RFP	6	2	0	1	1	0
	7	7	1	2	3	0
	8	3	0	2	2	0

[a] The IHC signal of PEDV antigen was scored as 0 to 3 according to the percentage of villous enterocytes within the section showing a positive signal. A score of 0 means that there were no positive cells, and scores of 1, 2, and 3 mean that <30%, 30 to 60%, and >60% of villous enterocytes showed a positive signal, respectively.

family of viruses that is devastating animal and human populations. It is possible that genetic manipulation of recombinant PEDVs will enable studies that can significantly enhance our understanding of the role of coronavirus genetics in the transmission, virulence, and pathologies that are central to both animal and human health and disease prevention.

In this article, we describe a reverse-genetics platform for a highly virulent U.S. PEDV strain that causes lethal disease in newborn piglets, allowing for the future identification of attenuating mutations and virulence alleles. In parallel, we have developed indicator viruses that can be used for high-throughput neutralization assays or to evaluate the impact of antivirals. This reverse-genetics system will allow for quick and robust PEDV genetic manipulation in a clinical North American isolate, allowing for in-depth study of viral replication and pathogenesis, which are essential for the development of safe and robust live attenuated-virus vaccines.

MATERIALS AND METHODS

Viruses and cells. The wild-type PC22A strain of PEDV (passage 4) was cultured on Vero cells, as described previously (25). Cells were grown in growth medium containing Dulbecco's modified Eagle medium (DMEM) (Life Technologies) supplemented with 5% fetal bovine serum (Life Technologies) and 1% antibiotic-antimycotic (Gibco). Virus was grown in Vero cells in maintenance medium, which was DMEM supplemented with 10 μg/ml trypsin (Life Technologies), 0.3% tryptose phosphate broth (Sigma), and 1% antibiotic-antimycotic (Life Technologies). Cells were kept in a humidified incubator at 37°C and 5% CO_2.

Assembly of full-length recombinant PEDV. The icPEDV clone was designed using six separate fragments (ordered from Bio Basic) flanked with unique flanking class II restriction sites that leave nonpalindromic overhangs. Sequences were ordered based on PC22A passage 4 sequence (GenBank accession number km392224.1). All cDNA subclones were grown in the pcXL-TOPO vector. In fragment E, a naturally occurring BsaI site was removed by introducing a silent mutation in order to prevent interference with assembly of the full-length infectious clone. All PEDV fragments were sequenced after transfection into bacterial culture to ensure sequence fidelity. The PEDV fragments were digested using restriction sites designated in Fig. 1, run on a 1% agarose gel, excised, and purified using a QIAquick gel extraction kit (Qiagen). The PEDV fragments were mixed and ligated overnight at 4°C using T4 DNA ligase (Roche). Ligated fragments were phenol-chloroform extracted, and full-length T7 RNA transcripts were generated as described in the mMessage mMachine manufacturer protocol (Ambion), but we allowed the reaction to run at 30°C for 3 h and then at room temperature for 2 h. In addition, SP6 PEDV-N gene transcripts were generated from the PCR-purified PEDV-N gene sample using a 4:1 ratio of cap to GTP (Ambion).

To generate the ORF3 deletion RFP construct, the tdTomato gene was amplified by PCR with flanking PEDV sequence and then inserted using native restriction sites into PEDV-F. PEDV-F-ΔORF3-RFP was cultured and sequenced to ensure seamless replacement of ORF3 with RFP containing the ORF3 TRS.

***In vitro* transfection.** Genome-length and N RNA transcripts were mixed with 800 μl of Vero-BI cells (1×10^7 cells/ml) in phosphate-buffered saline (PBS) and then added to an electroporation cuvette. Three pulses of 450 V at 50 μF were used to transfect the cells with a Gene Pulser II electroporator (Bio-Rad). The cells were allowed to recover for 10 min at room temperature and then were transferred to a 75-cm^2 flask in growth medium at 37°C for 2 h, after which time the cells were washed and incubated in cell culture medium. Trypsin was added to the culture at 5 μg/ml 12 h postelectroporation to assist in virus recovery and spread.

Sequence analysis identification of marker mutations. Virus harvested from small intestinal contents was grown in Vero-BI cell culture for 48 h. Virion RNA was harvested from the supernatant using the QIAamp viral RNA minikit (Qiagen). After purification, viral cDNA was generated with Superscript II reverse transcriptase (Life Technologies) as previously described by our group (26). To demonstrate the presence of the marker mutation, the icPEDV BsaI mutation site was amplified by PCR using primers 5′ TCCAAGCCATTTCTAGTTCTATT 3′ and 5′ TGACACAAC AAAGATGAGAACA 3′. PCR amplicons were gel purified and then sequenced using primers 5′ TCAGGCTAGCAGGAAGTTAG 3′ and 5′ AG GTCAACTAGTGTGTTGTTGATAT 3′.

Western blot and transcript analysis. Virus from infected animals was cultured in Vero-BI cell culture for 48 h and washed with PBS, and intracellular RNA was harvested from cells using NP-40 buffer (150 mM NaCl, 1% Triton X-100, 50 mM Tris, pH 8.0) for Western blots or TRIzol (Life Technologies) for RNA analysis. cDNA from viral RNA transcripts was generated using Superscript II reverse transcriptase (Life Technologies) and PCR amplified using primer pairs from the PEDV leader sequence and nucleocapsid gene. PCR products were separated on a 1% agarose gel and visualized on a Dark Reader transilluminator (Clare Chemical Research).

For Western blot analysis, protein from infected cells was denatured in 4× Laemmli buffer (Bio-Rad) at 95°C for 6 min and then separated on gradient 4 to 15% Mini-Protean precast gels (Bio-Rad) prior to electrophoretic transfer of the proteins to polyvinylidene difluoride (PVDF) membranes (Bio-Rad). To detect PEDV antigens, blots were first blocked with 5% milk in Tris-buffered saline with Tween 20 (TBST) and then probed with a polyclonal mouse serum (diluted 1:200) from mice which had been immunized with Venezuelan equine encephalitis virus replicon particles (VRP) expressing PEDV nucleocapsid (N) or spike (S) glycoprotein. Blots were developed using GE Healthcare Amersham ECL Western blotting detection reagents and exposed to film for imaging.

Animal studies. Four groups of 2- to 3-week-old gnotobiotic (Gn) pigs were used to examine the replication and pathogenesis of icPEDV- and icPEDV-ΔORF3-RFP-derived viruses *in vivo* and compared with PC22A- and mock-infected positive and negative controls, respectively (Table 1). Piglets were orally inoculated with 2 ml of icPEDV or icPEDV-ΔORF3-RFP culture supernatants after transfection (P0) ($<1.0 \times 10^2$ PFU/ml) or with the tissue culture-adapted PC22A strain at passage level 3 (P3) at a dose of 5.8 $\log_{10}$ PFU/pig. To investigate transmission, pigs 2, 5, 7, and 10 were cohoused in the same isolator as infected pigs but were separated by a stainless steel divider that contained small holes which allowed only indirect contact between the groups. Animals were monitored daily for clinical signs of disease, including diarrhea and vomiting. Rectal swabs were collected for scoring fecal denseness (scores: 0 = normal; 1 = pasty stool; 2 = semiliquid diarrhea; and 3 = liquid diarrhea) and for enumerating fecal viral RNA shedding by RT-quantitative PCR (RT-qPCR). Except for one pig in the icPEDV group, which was kept long term for the production of hyperimmune serum, the Gn pigs were euthanized at acute infection phase (within 5 days postinoculation [dpi] or 7 days postcontact with the inoculated pigs [dpc]) for histopathological examinations. At necropsy, small and large intestinal contents were collected and tested by RT-qPCR for viral RNA levels and for infectious virus by plaque assay. The different sections of the small intestine (duodenum, jejunum, ilium) and large intestine (cecum and colon) were collected for histopathological examination and stained with hematoxylin and eosin (H&E) stain. The derivation and maintenance of Gn pigs, sample collection and testing, and histopathology were performed as previously described (25, 57). All the animal use protocols employed in this study were reviewed and approved by the Agricultural Animal Care and Use Committee of The Ohio State University.

IHC staining. The immunohistochemistry (IHC) staining procedure was optimized as described previously (37) using the non-biotin-polymerized horseradish peroxidase (HRP) system (BioGenex Laboratories, San Ramon, CA). Briefly, intestinal tissue sections from each pig were deparaffinized and rehydrated in graded ethanol to PBS (pH 7.4). Antigen retrieval and unmasking were performed by treatment with 0.05% pronase E (Sigma-Aldrich, St. Louis, MO) for 20 min. The endogenous per-

oxidase activity was quenched with 3% hydrogen peroxide (Sigma) for 20 min. Then, the sections were incubated in Power Block solution (BioGenex) for 30 min at room temperature. Mouse monoclonal antibody anti-PEDV nucleocapsid protein (N) (SD6-29; a gift from E. Nelson and S. Lawson, South Dakota State University) was applied to each section at 4°C overnight. After two washes in PBS, a commercial Super Sensitive IHC detection system (BioGenex) was used. Finally, these sections were counterstained with Mayer's hematoxylin (BioGenex) and dehydrated, and coverslips were added. The IHC signal of PEDV antigen was scored as 0 to 3 according to the percentage of villous enterocytes within the section showing a positive signal. Scores were as follows: 0 indicated that there were no positive cells and 1, 2, and 3 indicated that <30%, 30 to 60%, and >60% of villous enterocytes showed a positive signal, respectively.

ACKNOWLEDGMENTS

We thank J. Hanson, R. Wood, and J. Ogg for animal care assistance, and T.Oka and X. Wang for technical assistance. Special thanks to Steven Lawson and Eric Nelson (Department of Veterinary and Biomedical Sciences, South Dakota State University) for providing mouse anti-PEDV nucleocapsid protein monoclonal antibody SD6-29.

Salaries and research support were provided by state and federal funds appropriated to Ohio Agricultural Research and Development Center (OARDC), The Ohio State University.

The authors acknowledge the key financial support from the National Institutes of Health, Center for Diagnostics and Discovery (U19 AI109761) to R.S.B. and Grant 2015-67015-23067 from the USDA to Q.W., L.S., and R.S.B.

REFERENCES

1. **Berry M, Gamieldien J, Fielding BC.** 2015. Identification of new respiratory viruses in the new millennium. Viruses **7:**996–1019. http://dx.doi.org/10.3390/v7030996.
2. **Stevenson GW, Hoang H, Schwartz KJ, Burrough ER, Sun D, Madson D, Cooper VL, Pillatzki A, Gauger P, Schmitt BJ, Koster LG, Killian ML, Yoon KJ.** 2013. Emergence of porcine epidemic diarrhea virus in the United States: clinical signs, lesions, and viral genomic sequences. J Vet Diagn Invest **25:**649–654. http://dx.doi.org/10.1177/1040638713501675.
3. **Madson DM, Magstadt DR, Arruda PHE, Hoang H, Sun D, Bower LP, Bhandari M, Burrough ER, Gauger PC, Pillatzki AE, Stevenson GW, Wilberts BL, Brodie J, Harmon KM, Wang C, Main RG, Zhang J, Yoon KJ.** 2014. Pathogenesis of porcine epidemic diarrhea virus isolate (US/Iowa/18984/2013) in 3-week-old weaned pigs. Vet Microbiol **174:**60–68. http://dx.doi.org/10.1016/j.vetmic.2014.09.002.
4. **Jung K, Annamalai T, Lu Z, Saif LJ.** 2015. Comparative pathogenesis of US porcine epidemic diarrhea virus (PEDV) strain PC21A in conventional 9-day-old nursing piglets vs. 26-day-old weaned pigs. Vet Microbiol **178:**31–40. http://dx.doi.org/10.1016/j.vetmic.2015.04.022.
5. **USDA-APHIS.** 2015. Swine enteric coronavirus diseases (SECD), including porcine epidemic diarrhea virus (PEDv). USDA, Animal and Plant Health Inspection Service. https://www.aphis.usda.gov/wps/portal/aphis/ourfocus/animalhealth?urile=wcm%3Apath%3A%2Faphis_content_library%2Fsa_our_focus%2Fsa_animal_health%2Fsa_animal_disease_information%2Fsa_swine_health%2Fct_ped_info. Accessed 1 July 2015.
6. **Ma Y, Zhang Y, Liang X, Lou F, Oglesbee M, Krakowka S, Li J.** 2015. Origin, evolution, and virulence of porcine deltacoronaviruses in the United States. mBio **6:**e00064. http://dx.doi.org/10.1128/mBio.00064-15.
7. **Thimmasandra Narayanappa A, Sooryanarain H, Deventhiran J, Cao D, Ammayappan Venkatachalam B, Kambiranda D, LeRoith T, Heffron CL, Lindstrom N, Hall K, Jobst P, Sexton C, Meng XJ, Elankumaran S.** 2015. A novel pathogenic mammalian orthoreovirus from diarrheic pigs and swine blood meal in the United States. mBio **6:**e00593-15. http://dx.doi.org/10.1128/mBio.00593-15.
8. **Vlasova AN, Marthaler D, Wang Q, Culhane MR, Rossow KD, Rovira A, Collins J, Saif LJ.** 2014. Distinct characteristics and complex evolution of PEDV strains, North America, May 2013–February 2014. Emerg Infect Dis **20:**1620–1628. http://dx.doi.org/10.3201/eid2010.140491.
9. **Abdul-Rasool S, Fielding BC.** 2010. Understanding human coronavirus HCoV-NL63. Open Virol J **4:**76–84.
10. **Song D, Park B.** 2012. Porcine epidemic diarrhoea virus: a comprehensive review of molecular epidemiology, diagnosis, and vaccines. Virus Genes **44:**167–175. http://dx.doi.org/10.1007/s11262-012-0713-1.
11. **Sun R-Q, Cai R-J, Chen Y-Q, Liang P-S, Chen D-K, Song C-X.** 2012. Outbreak of porcine epidemic diarrhea in suckling piglets, China. Emerg Infect Dis **18:**161–163. http://dx.doi.org/10.3201/eid1801.111259.
12. **Huang Y-W, Dickerman AW, Piñeyro P, Li L, Fang L, Kiehne R, Opriessnig T, Meng XJ.** 2013. Origin, evolution, and genotyping of emergent porcine epidemic diarrhea virus strains in the United States. mBio **4:**e00737-00713. http://dx.doi.org/10.1128/mBio.00737-13.
13. **Lin C-N, Chung W-B, Chang S-W, Wen C-C, Liu H, Chien C-H, Chiou M-T.** 2014. US-like strain of porcine epidemic diarrhea virus outbreaks in Taiwan, 2013–2014. J Vet Med Sci **76:**1297–1299. http://dx.doi.org/10.1292/jvms.14-0098.
14. **Song D, Moon H, Kang B.** 2015. Porcine epidemic diarrhea: a review of current epidemiology and available vaccines. Clin Exp Vaccine Res **4:**166–176. http://dx.doi.org/10.7774/cevr.2015.4.2.166.
15. **Liu C, Tang J, Ma Y, Liang X, Yang Y, Peng G, Qi Q, Jiang S, Li J, Du L, Li F.** 2015. Receptor usage and cell entry of porcine epidemic diarrhea coronavirus. J Virol **89:**6121–6125. http://dx.doi.org/10.1128/JVI.00430-15.
16. **Huan C-C, Wang Y, Ni B, Wang R, Huang L, Ren X-F, Tong G-Z, Ding C, Fan H-J, Mao X.** 2015. Porcine epidemic diarrhea virus uses cell-surface heparan sulfate as an attachment factor. Arch Virol **160:**1621–1628. http://dx.doi.org/10.1007/s00705-015-2408-0.
17. **Duarte M, Gelfi J, Lambert P, Rasschaert D, Laude H.** 1994. Genome organization of porcine epidemic diarrhoea virus. Adv Exp Med Biol **342:**55–60. http://dx.doi.org/10.1007/978-1-4615-2996-5_9.
18. **Sato T, Takeyama N, Katsumata A, Tuchiya K, Kodama T, Kusanagi K-I.** 2011. Mutations in the spike gene of porcine epidemic diarrhea virus associated with growth adaptation *in vitro* and attenuation of virulence *in vivo*. Virus Genes **43:**72–78. http://dx.doi.org/10.1007/s11262-011-0617-5.
19. **Park J-E, Cruz DJM, Shin H-J.** 2011. Receptor-bound porcine epidemic diarrhea virus spike protein cleaved by trypsin induces membrane fusion. Arch Virol **156:**1749–1756. http://dx.doi.org/10.1007/s00705-011-1044-6.
20. **Xu X, Zhang H, Zhang Q, Dong J, Liang Y, Huang Y, Liu H-J, Tong D.** 2013. Porcine epidemic diarrhea virus E protein causes endoplasmic reticulum stress and up-regulates interleukin-8 expression. Virol J **10:**26. http://dx.doi.org/10.1186/1743-422X-10-26.
21. **Xu X, Zhang H, Zhang Q, Huang Y, Dong J, Liang Y, Liu H-J, Tong D.** 2013. Porcine epidemic diarrhea virus N protein prolongs S-phase cell cycle, induces endoplasmic reticulum stress, and up-regulates interleukin-8 expression. Vet Microbiol **164:**212–221. http://dx.doi.org/10.1016/j.vetmic.2013.01.034.
22. **Kocherhans R, Bridgen A, Ackermann M, Tobler K.** 2001. Completion of the porcine epidemic diarrhoea coronavirus (PEDV) genome sequence. Virus Genes **23:**137–144. http://dx.doi.org/10.1023/A:1011831902219.
23. **Wang K, Lu W, Chen J, Xie S, Shi H, Hsu H, Yu W, Xu K, Bian C, Fischer WB, Schwarz W, Feng L, Sun B.** 2012. PEDV ORF3 encodes an ion channel protein and regulates virus production. FEBS Lett **586:**384–391. http://dx.doi.org/10.1016/j.febslet.2012.01.005.
24. **Li C, Li Z, Zou Y, Wicht O, van Kuppeveld FJM, Rottier PJM, Bosch BJ.** 2013. Manipulation of the porcine epidemic diarrhea virus genome using targeted RNA recombination. PLoS One **8:**e69997. http://dx.doi.org/10.1371/journal.pone.0069997.
25. **Oka T, Saif LJ, Marthaler D, Esseili MA, Meulia T, Lin C-M, Vlasova AN, Jung K, Zhang Y, Wang Q.** 2014. Cell culture isolation and sequence analysis of genetically diverse US porcine epidemic diarrhea virus strains including a novel strain with a large deletion in the spike gene. Vet Microbiol **173:**258–269. http://dx.doi.org/10.1016/j.vetmic.2014.08.012.
26. **Scobey T, Yount BL, Sims AC, Donaldson EF, Agnihothram SS, Menachery VD, Graham RL, Swanstrom J, Bove PF, Kim JD, Grego S, Randell SH, Baric RS.** 2013. Reverse genetics with a full-length infectious cDNA of the Middle East respiratory syndrome coronavirus. Proc Natl Acad Sci U S A **110:**16157–16162. http://dx.doi.org/10.1073/pnas.1311542110.
27. **Donaldson EF, Yount B, Sims AC, Burkett S, Pickles RJ, Baric RS.** 2008. Systematic assembly of a full-length infectious clone of human coronavirus NL63. J Virol **82:**11948–11957. http://dx.doi.org/10.1128/JVI.01804-08.
28. **Baric RS, Sims AC.** 2005. Development of mouse hepatitis virus and SARS-CoV infectious cDNA constructs. Curr Top Microbiol Immunol **287:**229–252.
29. **Yount B, Curtis KM, Fritz EA, Hensley LE, Jahrling PB, Prentice E,**

Denison MR, Geisbert TW, Baric RS. 2003. Reverse genetics with a full-length infectious cDNA of severe acute respiratory syndrome coronavirus. Proc Natl Acad Sci U S A **100:**12995–13000. http://dx.doi.org/10.1073/pnas.1735582100.

30. **Yount B, Curtis KM, Baric RS**. 2000. Strategy for systematic assembly of large RNA and DNA genomes: transmissible gastroenteritis virus model. J Virol **74:**10600–10611. http://dx.doi.org/10.1128/JVI.74.22.10600-10611.2000.
31. **Yount B, Denison MR, Weiss SR, Baric RS**. 2002. Systematic assembly of a full-length infectious cDNA of mouse hepatitis virus strain A59. J Virol **76:**11065–11078. http://dx.doi.org/10.1128/JVI.76.21.11065-11078.2002.
32. **Renukaradhya GJ, Meng X-J, Calvert JG, Roof M, Lager KM**. 2015. Live porcine reproductive and respiratory syndrome virus vaccines: current status and future direction. Vaccine **33:**4069–4080. http://dx.doi.org/10.1016/j.vaccine.2015.06.092.
33. **Schwegmann-Wessels C, Herrler G**. 2006. Transmissible gastroenteritis virus infection: a vanishing specter. Dtsch Tierarztl Wochenschr **113:**157–159.
34. **Pensaert M**. 1990. Background paper. The appearance of the porcine respiratory coronavirus has created new problems and perspectives. Adv Exp Med Biol **276:**419–420. http://dx.doi.org/10.1007/978-1-4684-5823-7_57.
35. **Wang L, Byrum B, Zhang Y**. 2014. Detection and genetic characterization of deltacoronavirus in pigs, Ohio, USA, 2014. Emerg Infect Dis **20:**1227–1230. http://dx.doi.org/10.3201/eid2007.140296.
36. **Jengarn J, Wongthida P, Wanasen N, Frantz PN, Wanitchang A, Jongkaewwattana A**. 2015. Genetic manipulation of porcine epidemic diarrhea virus (PEDV) recovered from a full-length infectious cDNA clone. J Gen Virol **96:**2206–2218. http://dx.doi.org/10.1099/vir.0.000184.
37. **Liu X, Lin C-M, Annamalai T, Gao X, Lu Z, Esseili MA, Jung K, El-Tholoth M, Saif LJ, Wang Q**. 2015. Determination of the infectious titer and virulence of an original US porcine epidemic diarrhea virus PC22A strain. Vet Res **46:**109. http://dx.doi.org/10.1186/s13567-015-0249-1.
38. **Herfst S, Imai M, Kawaoka Y, Fouchier RA**. 2014. Avian influenza virus transmission to mammals. Curr Top Microbiol Immunol **385:**137–155. http://dx.doi.org/10.1007/82_2014_387.
39. **Liu L, Lear Z, Hughes DJ, Wu W, Zhou EM, Whitehouse A, Chen H, Hiscox JA**. 2015. Resolution of the cellular proteome of the nucleocapsid protein from a highly pathogenic isolate of porcine reproductive and respiratory syndrome virus identifies PARP-1 as a cellular target whose interaction is critical for virus biology. Vet Microbiol **176:**109–119. http://dx.doi.org/10.1016/j.vetmic.2014.11.023.
40. **USDA-APHIS.** 2014. USDA licenses first vaccine for porcine epidemic diarrhea. USDA Animal and Plant Health Inspection Service, Veterinary Services, Washington, DC.
41. **Zoetis.** 2014. USDA grants Zoetis a conditional license for porcine epidemic diarrhea vaccine. Zoetis, Florham Park, NJ. https://www.zoetis.com/news-media/feature-stories/usda-grants-zoetis-conditional-license-porcine-epidemic-diarrhea-vaccine.
42. **Hart MK, Caswell-Stephan K, Bakken R, Tammariello R, Pratt W, Davis N, Johnston RE, Smith J, Steele K**. 2000. Improved mucosal protection against Venezuelan equine encephalitis virus is induced by the molecularly defined, live-attenuated V3526 vaccine candidate. Vaccine **18:**3067–3075. http://dx.doi.org/10.1016/S0264-410X(00)00042-6.
43. **Fine DL, Roberts BA, Teehee ML, Terpening SJ, Kelly CLH, Raetz JL, Baker DC, Powers AM, Bowen RA**. 2007. Venezuelan equine encephalitis virus vaccine candidate (V3526) safety, immunogenicity and efficacy in horses. Vaccine **25:**1868–1876. http://dx.doi.org/10.1016/j.vaccine.2006.10.030.
44. **Rao V, Hinz ME, Roberts BA, Fine D**. 2004. Environmental hazard assessment of Venezuelan equine encephalitis virus vaccine candidate strain V3526. Vaccine **22:**2667–2673. http://dx.doi.org/10.1016/j.vaccine.2003.09.041.
45. **Tonkin DR, Whitmore A, Johnston RE, Barro M**. 2012. Infected dendritic cells are sufficient to mediate the adjuvant activity generated by Venezuelan equine encephalitis virus replicon particles. Vaccine **30:**4532–4542. http://dx.doi.org/10.1016/j.vaccine.2012.04.030.
46. **MacDonald GH, Johnston RE**. 2000. Role of dendritic cell targeting in Venezuelan equine encephalitis virus pathogenesis. J Virol **74:**914–922. http://dx.doi.org/10.1128/JVI.74.2.914-922.2000.
47. **Zhao J, Li K, Wohlford-Lenane C, Agnihothram SS, Fett C, Zhao J, Gale MJ, Jr, Baric RS, Enjuanes L, Gallagher T, McCray PB, Jr, Perlman S**. 2014. Rapid generation of a mouse model for Middle East respiratory syndrome. Proc Natl Acad Sci U S A **111:**4970–4975. http://dx.doi.org/10.1073/pnas.1323279111.
48. **Agnihothram S, Yount BL, Jr, Donaldson EF, Huynh J, Menachery VD, Gralinski LE, Graham RL, Becker MM, Tomar S, Scobey TD, Osswald HL, Whitmore A, Gopal R, Ghosh AK, Mesecar A, Zambon M, Heise M, Denison MR, Baric RS**. 2014. A mouse model for betacoronavirus subgroup 2c using a bat coronavirus strain HKU5 variant. mBio **5:**e00047-14. http://dx.doi.org/10.1128/mBio.00047-14.
49. **Sheahan T, Whitmore A, Long K, Ferris M, Rockx B, Funkhouser W, Donaldson E, Gralinski L, Collier M, Heise M, Davis N, Johnston R, Baric RS**. 2011. Successful vaccination strategies that protect aged mice from lethal challenge from influenza virus and heterologous severe acute respiratory syndrome coronavirus. J Virol **85:**217–230. http://dx.doi.org/10.1128/JVI.01805-10.
50. **Graham RL, Becker MM, Eckerle LD, Bolles M, Denison MR, Baric RS**. 2012. A live, impaired-fidelity coronavirus vaccine protects in an aged, immunocompromised mouse model of lethal disease. Nat Med **18:**1820–1826. http://dx.doi.org/10.1038/nm.2972.
51. **Menachery VD, Yount BL, Jr, Josset L, Gralinski LE, Scobey T, Agnihothram S, Katze MG, Baric RS**. 2014. Attenuation and restoration of severe acute respiratory syndrome coronavirus mutant lacking 2′-o-methyltransferase activity. J Virol **88:**4251–4264. http://dx.doi.org/10.1128/JVI.03571-13.
52. **Regla-Nava JA, Nieto-Torres JL, Jimenez-Guardeño JM, Fernandez-Delgado R, Fett C, Castaño-Rodríguez C, Perlman S, Enjuanes L, DeDiego ML**. 2015. Severe acute respiratory syndrome coronaviruses with mutations in the E protein are attenuated and promising vaccine candidates. J Virol **89:**3870–3887. http://dx.doi.org/10.1128/JVI.03566-14.
53. **Graham RL, Baric RS**. 2010. Recombination, reservoirs, and the modular spike: mechanisms of coronavirus cross-species transmission. J Virol **84:**3134–3146. http://dx.doi.org/10.1128/JVI.01394-09.
54. **Denison MR, Graham RL, Donaldson EF, Eckerle LD, Baric RS**. 2011. Coronaviruses: an RNA proofreading machine regulates replication fidelity and diversity. RNA Biol **8:**270–279. http://dx.doi.org/10.4161/rna.8.2.15013.
55. **Yount B, Roberts RS, Lindesmith L, Baric RS**. 2006. Rewiring the severe acute respiratory syndrome coronavirus (SARS-CoV) transcription circuit: engineering a recombination-resistant genome. Proc Natl Acad Sci U S A **103:**12546–12551. http://dx.doi.org/10.1073/pnas.0605438103.
56. **Gralinski LE, Baric RS**. 2015. Molecular pathology of emerging coronavirus infections. J Pathol **235:**185–195. http://dx.doi.org/10.1002/path.4454.
57. **Jung K, Wang Q, Scheuer KA, Lu Z, Zhang Y, Saif LJ**. 2014. Pathology of US porcine epidemic diarrhea virus strain PC21A in gnotobiotic pigs. Emerg Infect Dis **20:**668–671. http://dx.doi.org/10.3201/eid2004.131685.